ResearchGate

See discussions, stats, and author profiles for this publication at: https://www.researchgate.net/publication/258188214

High Temperature Solid–Solid Transition in Ammonium Chloride Confined to Nanopores

ARTICLE *in* THE JOURNAL OF PHYSICAL CHEMISTRY C · JUNE 2013

Impact Factor: 4.77 · DOI: 10.1021/jp403910f

CITATIONS
7

READS
65

3 AUTHORS:

Reza Farasat
Tulane University
4 PUBLICATIONS **10** CITATIONS
SEE PROFILE

Benjamin Yancey
University of Alabama at Birmingham
12 PUBLICATIONS **27** CITATIONS
SEE PROFILE

Sergey Vyazovkin
University of Alabama at Birmingham
162 PUBLICATIONS **9,712** CITATIONS
SEE PROFILE

Available from: Benjamin Yancey
Retrieved on: 24 January 2016

THE JOURNAL OF PHYSICAL CHEMISTRY C

Article

pubs.acs.org/JPCC

High Temperature Solid−Solid Transition in Ammonium Chloride Confined to Nanopores

Reza Farasat, Benjamin Yancey, and Sergey Vyazovkin*

Department of Chemistry, University of Alabama at Birmingham, 901 S. 14th Street, Birmingham, Alabama 35294, United States

ABSTRACT: This paper describes a calorimetric (DSC) study of the high temperature (~190 °C) solid−solid phase transition in ammonium chloride in silica nanopores (4−30 nm) and in bulk. The study focuses on the values of the transition heat and temperature as well as on the transition kinetics. Because ammonium chloride is loaded from a solution, the pores are only filled partially. Thermogravimetric analysis is employed to evaluate the pore fullness, which is further used to estimate the height of ammonium chloride layer deposited inside the pores. With increasing the layer height, the heat of transition increases toward the bulk value. Relative to the bulk value, the transition temperature measured on heating and on cooling respectively increases and decreases with decreasing the layer height. In larger pores (15 and 30 nm), the transition has revealed a second DSC peak that appears above 210 °C on heating and below 100 °C on cooling. The temperature dependencies of the effective activation energy derived from isoconversional kinetic analysis of DSC data have been parametrized in terms of the Turnbull−Fisher model. It is found that the transition in the pores encounters a larger free energy barrier to nucleation.

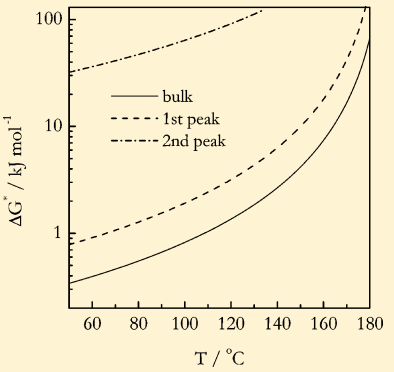

1. INTRODUCTION

The thermal behavior of systems dimensionally reduced to nanometer sizes is a topic of great fundamental significance and practical relevance. Although much of research effort has been focused on the phase transitions in nanoconfined systems, the focus has primarily been on melting−crystallization[1] and glass transitions.[2] Two reviews[1,2] published about a decade ago had included several hundred references on these types of transitions. The literature on solid−solid phase transitions has been far scarcer. Of course, the solid−solid phase transitions are not as abundant as the transitions between the solid, melt, and glass phases. However, they are just as important because they affect a variety of magnetic, electrical, mechanical, and optical properties as well as chemical reactivity and biological activity. For this reason, nanoconfinement as a means of controlling phase transitions also provides a tool for controlling a host of practically important physical properties of solids.

Some of the studies of nanoconfinement in the solid−solid transitions have been performed on compounds that are either gases or liquids at ambient temperatures. Examples are the solid−solid transitions in frozen oxygen[3] and cyclohexane[4] in porous silica glasses. If gases and liquids tend to enter the pores spontaneously, the substances that are solid at normal conditions need to be either melted or dissolved to penetrate a porous matrix. The melt route has been applied to study the solid−solid transitions in sodium nitrite,[5−9] sodium nitrate,[9] and potassium dihydrogen phosphate.[10] The solution route has not been as common but has been utilized[11] to examine the melting and solid−solid transition in sodium nitrate. Although the melt route is likely to produce completely filled pores, it is not suitable for "gentle" compounds that would degrade before or during melting. The solution route is much more delicate but unavoidably leads to pores that are partially filled because the solute constitutes only a fraction of solution. The extent of pore fullness can be increased through multiple loadings. A model linking the extent of fullness to the solution concentration and number of loadings has recently been proposed by us.[12] However, even after several loadings the dimensions of solid phase formed would typically be markedly smaller than the size of the pores.

Depending on the strength of interaction between the constituents (i.e., ions or molecules) of the solid and the pore wall, one can picture two limiting cases. First, if the interaction is negligibly weak, the solid would tend to form isolated particles inside the pores. Second, if the interaction is strong, the solid would form a layer on the surface of the pore walls. The pore wall surface in silica is very electrostatically active. In addition to SiO dipoles, it contains surface silanol groups that ionize to $Si-O^-$ and thus can engage in a variety of interactions depending on the type of species introduced in the pores. Note that the solid−solid transitions in the pores have been studied for two major types of solids: molecular[3,4] and ionic.[5−10] Molecules can interact with the surface via relatively weak van der Waals and dipole−dipole forces. If a molecule is polar or capable of hydrogen bonding, it can engage in stronger ion-dipole or hydrogen-bonding interaction with the surface. Ions, on the other hand, can interact very strongly by forming ionic compounds (i.e., $Si-O^-NH_4^+$)[13] and coordination complexes with the Si−O−Si oxygen atoms.[14]

Received: April 19, 2013
Revised: June 10, 2013

 © XXXX American Chemical Society dx.doi.org/10.1021/jp403910f | J. Phys. Chem. C XXXX, XXX, XXX−XXX

Considering the difference in the strength of interaction between the silica surface and molecular or ionic solids, their respective studies can highlight two different aspects of nanoconfinement: the effect of the size of confined solid and the effect of interaction with confining surface. The present study is intended to highlight the surface interaction effect by calorimetric measurements of the temperature, heat, and kinetics of the high temperature solid−solid transition in ammonium chloride loaded in silica nanopores. The compound has two solid−solid transitions, which reportedly[15] occur at −31 and 196 °C. Unlike the transition at −31 °C, the high temperature transition from form II to form I is accompanied by a significant heat of transition, which makes it convenient to study. One of the important reasons to use ammonium chloride is that on heating to 400 °C it decomposes entirely into gases[16] which allows one to employ thermogravimetric analysis[17] for accurate determination of its mass loaded in silica.[12] In addition, this compound is well soluble in water which affords significant variability in terms of the amount loaded into the silica pores. Finally, we are not aware of any existing studies of this phase transition under the conditions of nanoconfinement.

2. EXPERIMENTAL SECTION

ACS reagent grade ammonium chloride was purchased from Aldrich and recrystallized before use. The saturated solutions were prepared by using deionized water in accord with the respective values of the solubility (37 g per 100 cm^3 of water at 25 °C).[18] The 50 and 25% diluted solutions were prepared by respectively taking 2 and 4 times less solute than required by the solubility. The solutions were used to load the salt into the pores of the silica gel samples (SiliaFlash) that were generously supplied by SiliCycle Inc. (Quebec City, Canada). The samples were in the form of powder having narrow size distribution (40−63 μm) and nominal pore diameters of 4, 6, 9, 15, and 30 nm. The actual values of the pore diameters as well as surface area and pore volume as determined by nitrogen adsorption were provided by the manufacturer (Table 1). Although

Table 1. Basic Parameters of the Silica Samples Used

	actual values		
nominal pore diam (nm)	pore diam (nm)	surface area (m^2 g^{-1})	pore vol (cm^3 g^{-1})
4	3.9	598	0.60
6	5.7	496	0.71
9	10.0	358	0.89
15	16.7	285	1.19
30	28.4	175	1.24

throughout the paper we refer to the pore diameters by their nominal diameters, all calculations were performed by using the actual values. Loading was performed by immersing silica into the salt solutions for 2 h. After that, the solution was carefully separated from the silica samples which were transferred onto filter paper to remove excess of the solution. The loaded samples were then dried in an oven at 140 °C for 1 h. For multiple loadings the dried samples were again subjected to the same loading procedure. Single load was applied to samples of all pores sizes. In addition, the samples of pores sizes 6, 15, and 30 nm were loaded up to 3 times. The 30 nm samples were also prepared by loading once from 50% and 25% solutions. The mass of loaded ammonium chloride was evaluated thermogravimetrically. The details of the procedure and examples are given in our previous work.[12]

All calorimetric measurements were taken with a heat flux DSC (Mettler-Toledo, 823e). Indium and zinc standards were used to perform temperature, heat flow, and tau-lag calibrations. The experiments were conducted in the atmosphere of nitrogen flow (80 mL min^{-1}). The samples were run in closed 100 μL aluminum pans. The sample mass of neat ammonium chloride was ∼5 mg. The mass of silica samples loaded with ammonium chloride was varied in the range 15−30 mg to keep the mass of ammonium chloride in the pores close to 5 mg. The values of the heat and temperature of the transition were measured on heating and cooling at a rate 10 °C min^{-1}. The values were estimated as the mean of three repetitive measurements. As a control, similar runs were performed on a mechanical mixture of silica and ammonium chloride and found to yield the heat and temperature of the transition, which are practically identical to those for neat ammonium chloride. For kinetic calculations the measurements were carried out at the cooling rates 2, 3, 4.5, 6.75, and 10 °C min^{-1}.

3. RESULTS AND DISCUSSION

Basic Equations. As discussed in the Introduction, loading of ammonium chloride from an aqueous solution into the silica pores should yield a layer of the solid attached to the pore walls. In this circumstance, the pore diameter, routinely used to characterize nanoconfinement in completely filled pores, becomes practically irrelevant because the layer height would change with the pore fullness. On the other hand, the pore fullness that can be evaluated via mass gain measurements would be a suitable measure of nanoconfinement only when using one silica sample of certain pore diameter. However, the same pore fullness in silica samples having different pore diameters would result in respectively different layer heights. Therefore, a much more relevant parameter for exploring nanoconfinement in the silica pores partially filled with an ionic solid is the layer height. This parameter, h, can be estimated as follows[12]

$$h = r_0(1 - \sqrt{1 - \Theta}) \quad (1)$$

where r_0 is the pore radius and Θ is the pore fullness. Equation 1 is derived under the assumption of cylindrical pores. This assumption is commonly made in numerous simulations.[1,2] It is justified by extensive microscopic studies that indicate that the silica gel pores have the structure of interconnected (necked) globules, which is best approximated as a network of cylindrical pores.[19,20] The pore fullness is defined as the ratio of the volume filled to the volume available:

$$\Theta = \frac{\Delta m/\rho}{PM} \quad (2)$$

where Δm is the mass (g) of the solute deposited in the pores after removing the solvent or simply a mass gain, ρ is the solute density (g cm^{-3}), P is the pore volume per unit mass (cm^3 g^{-1}), and M is the mass (g) of the porous material. Although the pore fullness attained on a single loading, Θ_1, is limited by the ratio of the saturated solution concentration to the solute density, it can be increased to Θ_n through repetitive number loadings, n, in accord with[12]

$$\Theta_n = 1 - (1 - \Theta_1)^n \quad (3)$$

dx.doi.org/10.1021/jp403910f | J. Phys. Chem. C XXXX, XXX, XXX−XXX

It follows from eqs 1 and 3 that the layer height can be controlled by controlling the values of Θ and n. For a single load (n = 1) from a saturated solution, the maximum theoretical Θ value equals $\Theta_1 \sim 0.24$.[12] Then, depending on the pore radius (Table 1), this type of loading into the samples used in the present study should yield (eq 1) the layer heights ranging from 0.3 to 1.8 nm. Because multiple loadings ($n > 1$) from a saturated solution allow the Θ value to be raised above Θ_1 (eq 3), the application of this approach to the largest pore sizes (i.e., 30 nm) can yield (eq 1) the layer heights larger than 1.8 nm. On the other hand, a single load from a diluted solution would give rise to the Θ value smaller than Θ_1 and, thus, smaller layer heights.

In this work, the actual pore fullness has been determined by eq 2, where Δm is evaluated thermogravimetrically, P is taken from Table 1, the ammonium chloride density is 1.51[18] g cm^{-3}, and M is measured by an analytical balance. Then eq 1 has been used to estimate the layer height.

General Results. According to our repetitive measurements performed on three samples of bulk ammonium chloride, the transition from the form II to I starts at 189.6 ± 0.7 °C (extrapolated onset of the DSC peak). On heating at 10 °C min^{-1} DSC peak reaches a maximum at T_p = 192.4 ± 0.8 °C (peak temperature). On cooling, the transition from the form I to II peaks at 160.8 ± 0.6 °C. The absolute value of the transition heat averaged over heating and cooling scans is determined to be 85 ± 4 J g^{-1}. The transition from the form II to I has been previously reported to occur at 185 °C[21] (unspecified point of a DTA peak, heating rate 0.25 °C min, 7 g sample) and at T_p = 189 ± 1 °C[22] (heating rate 1 °C min, 7 mg sample). The T_p values for both heating and cooling have been reported[23] as 196 °C (form II to I) and 161 °C (form I to II) for unspecified heating/cooling rate and sample mass. The same work[23] also reports two values of the transition heat 83 and 88 J g^{-1} (15% uncertainty) depending on particle size.

Figure 1 demonstrates some typical DSC data obtained for heating scans of ammonium chloride in its bulk form as well as in silica pores. This graph illustrates well our earlier point that the pore diameter is an irrelevant parameter in the case of partially filled pores. As one can see, the largest T_p value (~196 °C) is detected in 4 nm pores single loaded from the saturated solution. However, a similar value is found in 30 nm pores single loaded from 25% solution. On the other hand, the transition in 30 nm pores triple loaded from the saturated solution demonstrates the lowest value (~192 °C) which is similar to that in the bulk. If the data are looked at from the standpoint of the estimated layer height, it is clear that the largest T_p value is observed in the thinnest layers (Figure 1).

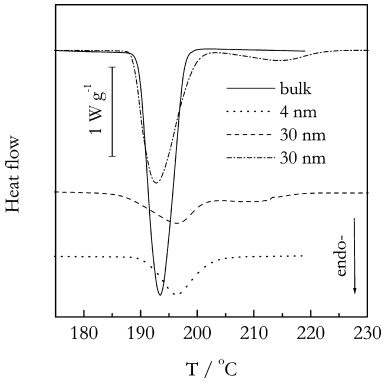

Figure 1. DSC curves measured at heating rate 10 °C min^{-1} for bulk and silica loaded (dash-dotted line: 30 nm pores triple loaded from saturated solution, estimated h = 5.3 nm; dashed line: 30 nm single loaded from 25% solution, estimated h = 0.3 nm; dotted line: 4 nm single loaded from saturated solution, estimated h = 0.2 nm) samples.

This figure also demonstrates some general trends found in the systems studied. Generally, the transition in the pores differs in both position and shape of the DSC peak. The peaks become broader and shorter, indicating that the process in the pores is slower. They also become asymmetrical, revealing some extent of tailing that may be a sign of diffusional retardation taking place at later stages of the transition. The peak position shifts to higher temperatures on heating and to lower temperatures on cooling. The existence of the extra superheating or supercooling suggests again that the process in the nanopores is more kinetically hindered than in the bulk. While different in extent, these two effects have been common for all confined systems studied in the present work.

Another effect has been observed (Figure 1) only in 30 nm pores at all types of loadings (i.e., single loadings from saturated and diluted solutions as well as multiple loadings from saturated solution) and in 15 nm pores at multiple loadings. The effect consists in the appearance of a second peak. The peak is as broad as the first one but much shorter. On average its area is about one-tenth of that for the first peak. Relative to the first peak, the second one is shifted by ~10−40 °C to higher temperatures on heating and by 30−90 °C to lower temperatures on cooling. We hypothesize that the second peak is probably associated with the formation of small amounts of a second phase, the transition of which is even more kinetically hindered than in the regular nanoconfined phase represented by either the first or the single peak. Some insights into the possible origin of this phase and specificity of its transition are provided later. For now, it is a worthy of note that the formation of unusual crystalline polymorphs in nanopores has been reported[24−27] for a number of molecular solids.

Heats of Transition. Figure 2 presents the values of endothermic heat of transition as a function of the estimated layer height. For those systems that reveal two DSC peaks on transition, the heat of transition was determined by the total area of both peaks. The absolute heats of transition measured

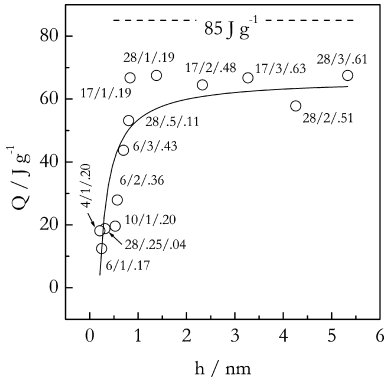

Figure 2. Endothermic heat of transition measured at heating rate 10 °C min^{-1} vs layer height (solid line is a fit to eq 8). Numbers by the points represent pore diameter (Table 1)/number of loadings/pore fullness. Fractional number of loadings 0.25 and 0.5 stand respectively for single loading from 25% and 50% diluted solution. The same systems are shown in Figures 3−5.

dx.doi.org/10.1021/jp403910f | J. Phys. Chem. C XXXX, XXX, XXX−XXX

calorimetrically were divided over the mass of actually loaded ammonium chloride evaluated thermogravimetrically. Thus, the resulting thermal effects can be expected to be of similar value as in the bulk, i.e., ~85 J g^{-1} unless the nanoporous medium modifies the transition.

The data presented in Figure 2 support our earlier point that when describing the behavior of systems in partially filled nanopores, the estimated layer height is more relevant parameter than either pore size or pore fullness. The heat of transition increases dramatically with increasing the layer height until the latter reaches ~1 nm. After that the heat value plateaus at ~67 J g^{-1}, i.e., ~18 J g^{-1} lower than the expected bulk value. This behavior can be explained by some fraction of the mass loaded being inactive, i.e., not participating in the transition. Considering the strong interactions between ammonium cations and the silica surface, we can expect at least one ionic layer of absorbed ammonium chloride not to participate in the phase transition. The data presented in Figure 2 indicate that the initial increase of the heat of transition occurs almost linearly with the layer height at approximately 50−60 J g^{-1} per 1 nm. Then, the ~18 J g^{-1} difference between the plateau and bulk value corresponds to the inactive ionic layer whose height is roughly a little over 0.3 nm. This value is quite similar to the diameter of an ammonium ion, 0.28 nm.[28]

The idea of some fraction of the mass loaded being inactive can be presented in the form of a simple equation

$$Q = Q_B\left(1 - \frac{m_0}{m}\right) \tag{4}$$

where m is the mass loaded, m_0 is the inactive mass, and Q_B is the heat of transition for the bulk substance. Considering that the layer height increases proportionally to the mass loaded, we can try to replace the masses with respective heights and derive an equation that describes the dependence observed in Figure 2. Such an equation can be derived by making some simple assumptions. First, assuming that density of the substance does not change with the layer height, eq 4 can be converted to

$$Q = Q_B\left(1 - \frac{V_0}{V}\right) \tag{5}$$

where V is the volume of deposited layer and V_0 is the inactive volume of this layer. Second, we can assume that the pores are approximately cylindrical. Then, the volume of the layer deposited on the walls of a cylinder can be defined as the difference between the total volume of the pore and the volume of the unfilled part:

$$\pi r^2 l - \pi(r - h)^2 l = \pi l(2rh - h^2) \tag{6}$$

Subject to eq 6, eq 5 can written as

$$Q = Q_B\left(1 - \frac{2rh_0 - h_0^2}{2rh - h^2}\right) \tag{7}$$

Now assuming that h^2 and ${h_0}^2$ can be respectively neglected relative to $2rh$ and $2rh_0$, eq 7 can be approximated as

$$Q \approx Q_B\left(1 - \frac{h_0}{h}\right) \tag{8}$$

The relative error of such approximation can be estimated as

$$\left|\frac{\frac{V_0}{V} - \frac{h_0}{h}}{\frac{V_0}{V}}\right| = \left|\frac{h - h_0}{2r - h_0}\right| \tag{9}$$

The error increases with increasing the deposited layer height (h) and decreasing the pore diameter ($2r$). Assuming that h_0 is around 0.2−0.3 nm and substituting the actual values of the pore diameters and values of h accomplished on loading, we find that the average absolute error in eq 8 is only 7%.

The results of fitting the transition heat vs the layer height data are shown in Figure 2. While not perfect, the fit demonstrates the correlation coefficient, ρ = 0.871, which is statistically significant at the 95% level confidence (the critical ρ value is 0.602).[29] The estimated value of the inactive layer height, h_0, is 0.20 ± 0.02 nm, which is roughly similar to the value estimated from the difference between the plateau and bulk values of the transition heat. The estimated value of Q_B is 66 ± 5 J g^{-1}, which is noticeably lower than the actually measured bulk value. Setting Q_B to 85 J g^{-1} and varying h_0 to fit the same data does not much affect the estimated value of h_0. The resulting inactive layer height becomes 0.23 ± 0.03 nm, whereas the correlation coefficient drops to 0.659, which remains statistically significant. On the other hand, a statistical test suggests that a decrease in ρ from 0.871 to 0.659 is statistically insignificant. This means that statistically we cannot rule out the possibility that the heat of transition may asymptotically reach the bulk value as the layer height continues to increase.

Figure 3 displays the exothermic heats of the reverse transition measured on cooling. It is seen that the heat of transition increases significantly with the layer height. The observed trend is similar to that seen on heating (Figure 2). Most of the increase occurs within first 1−1.5 nm, past which the value practically levels off at ~77 J g^{-1}, which is noticeably lower than the value measured for the bulk sample. Fitting the data to eq 8 demonstrates statistically significant correlation with the following parameters: Q_B = 75 ± 6 J g^{-1} and h_0 = 0.22 ± 0.02 nm.

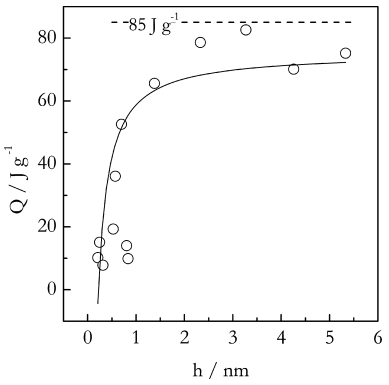

Figure 3. Exothermic heat of transition measured at cooling rate 10 °C min^{-1} vs layer height (solid line is a fit to eq 8).

Overall, for both heating and cooling data we see that the absolute value of the transition heat increases with the layer height. In either case, the behavior can be explained by the presence of an inactive layer whose size is estimated to be close to a single layer of ammonium ions. This behavior is similar to that reported in the literature for fully filled pores. In the latter case, the heat of transition is generally smaller than in the bulk

dx.doi.org/10.1021/jp403910f | J. Phys. Chem. C XXXX, XXX, XXX−XXX

but increases to the bulk value as the pore size increases. For instance, the heat of transition in $NaNO_2$ confined to 7 nm pores has been observed to be less than 10% of the bulk value.[8] While not quantified, a significant decrease in the heat of transition has been mentioned for $NaNO_2$ and $NaNO_3$ in 23 and 160 nm pores. The heat of the solid−solid phase transition in cyclohexane in nanopores has been reported[4] to increase with the pores size being 36% and 63% of the bulk value in 4 and 7.5 nm pores. The bulk value was reached only when the pore size exceeded 60 nm. Note that for solid−solid transitions the effect appears similar to that reported[30] for the heat of melting of seven organic liquids frozen in organically modified porous glasses. For instance, in 4 nm pores the measured value varied from 28% to 57% of the bulk value depending on the liquid. Even in 8.5 nm pores the heats of melting were in the range 50−88% of the bulk value.

Temperatures of Transition. Figures 4 and 5 show how the T_p values (i.e., DSC peak positions) measured on heating and cooling change with respect to estimated layer height. Simple behavior is observed for the first peak in both sets of measurements. On heating (Figure 4), all the peak temperatures are above the bulk value. The deviations are relatively small and do not exceed 4 °C. However, they demonstrate a systematic trend so that the peak temperature decreases with increasing the layer height. The strength of this correlation has been estimated by calculating the Spearman's rank correlation coefficient, whose value is 0.761. The value is statistically significant at a 95% confidence level. On cooling (Figure 5), all T_p values for the first peak fall below the bulk value. The values clearly increase with increasing the layer height rising toward the bulk value. The relationship is statistically significant with the Spearman's correlation coefficient 0.900. By pulling together the results presented in Figures 4 and 5, we can state that as the layer height decreases, the temperature of the transition in the pores deviates increasingly from that in the bulk. In other words, as the layer height becomes smaller, the transition requires larger superheating on heating and larger supercooling on cooling.

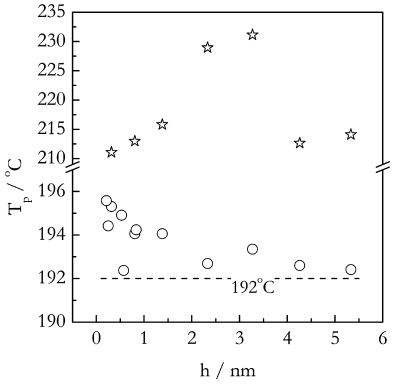

Figure 4. Transition peak temperature measured at heating rate 10 °C min^{-1} (circles: first peak; stars: second peak; dashed line: bulk T_p value).

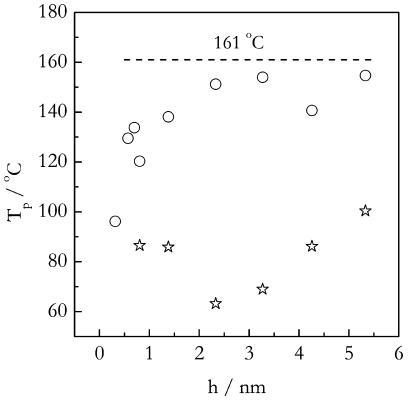

Figure 5. Transition peak temperature measured at cooling rate 10 °C min^{-1} (circles: first peak; stars: second peak; dashed line: bulk T_p value).

A distinct difference between the transitions on cooling and heating is that the former demonstrates far bigger temperature deviations than the latter. Apparently the transition from the form II to I (i.e., on heating) is thermodynamically limited, i.e., occurs quickly just past the critical temperature. On the contrary, the reverse transition (i.e., on cooling) appears to be driven by the slow kinetics of nucleation. That is, the situation is reminiscent of the solid−liquid (melting) and liquid−solid (crystallization) transitions.

As mentioned earlier, our dependence of the transition heat on the layer height is similar to what is typically reported in the literature. This however does not apply to the aforediscussed dependence of the temperature on the layer height. The available literature on the solid−solid transitions in the fully filled pores usually reports the opposite dependence, i.e., a decrease in the transition temperature with decreasing the pore size. This trend has been well established for molecular solids. The temperature for the solid−solid transition in oxygen has been discovered[3] to drop sequentially in 20, 5, and 2 nm pores by respectively 2, 5, and 10 °C relative to the bulk value, −229 °C. Similarly, for cyclohexane (bulk transition temperature −87 °C) the transition temperature has been determined to fall successively in 30, 15, 7.5, and 4 nm pores by 2, 3, 8, and 10 °C, respectively. It should be noted that these effects have been obtained for molecular solids that, as stated earlier, tend to have relatively weak interactions with silica surface.

For ionic solids the effect is not clear-cut. For $NaNO_2$ (bulk transition temperature ∼164−165 °C) confined to 30−80 nm pores of synthetic opal the transition occurred at 1 °C lower on heating and 11 °C lower on cooling comparative to the respective bulk values.[5] For the same salt loaded in 7 nm pores the transition temperature has been reported[8] to drop by 22 °C below the bulk. In 23 nm pores the transition temperature of $NaNO_2$ is found[9] to be 3−4 °C below the bulk value, whereas for $NaNO_3$ (bulk transition temperature ∼275 °C) is only 1 °C lower than in the bulk. On the other hand, some publications report that the temperature shift for the transition in $NaNO_2$ is either very small (7 nm pores)[6] or absent[31] (5−20 nm pores or particles). It does not seem illogical to suggest that the absence of a clear-cut decrease of the transition temperature in the nanopores might be due to an overlap of the size and surface effects that pull respectively in the opposite directions. In other words, if diminishing the size tends to lower the transition temperature, the strong interaction with the silica surface tends to increase it. It should also be noted that in our systems the layer height is less than 6 nm, and the largest increase is seen below 2 nm. However, in the aforementioned fully filled pores the smallest size of the solid phase is the same as the size of the smallest pores, i.e., 7 nm. Needless to say, that with increasing the size the surface effect contribution becomes smaller (Figure 4), and it may become outweighed by the size effect causing the

dx.doi.org/10.1021/jp403910f | J. Phys. Chem. C XXXX, XXX, XXX−XXX

transition temperature to drop below the bulk values. Unfortunately, there is no simple way to fill silica pores completely with ammonium chloride to test this idea. It is something that should further be tested on an ionic compound that can be easily loaded from the melt as well as from a solution.

For salts, we are only aware of a single case that demonstrates[6] a significant increase (≥7 °C) for the solid−solid transition in KH_2PO_4 (bulk transition temperature ca. −150 °C) confined to 7−100 nm pores. On the other hand, there are several known cases of an increase in the melting temperature with decreasing the dimensions of substances nanoconfined in matrices. The examples include indium[32] and lead[33] in aluminum matrix and benzene[34] and carbon tetrachloride[35] in graphitic nanopores. According to simulations by Miyahara and Gubbins,[36] the increase is to be expected when the strength of the attractive interactions between confined molecules and confining surface is larger than that for confined molecules themselves. Considering the high strength of interaction between ammonia ions and silica surface, this result[36] certainly lends some theoretical support to the effect observed in the present study. Nonetheless, one should not generally disregard the role of an anion, whose interaction with a cation and/or the confining surface may weaken the strength of the cation−surface interaction and thus affect the direction, in which the transition temperature shifts relative to the bulk value.

Regarding the position of the second peak, variation of the T_p values with the layer height does not demonstrate either systematic increase or decrease expected from the theoretical considerations. One the other hand, the amount of data is insufficient to test statistically whether the dependence is random. It is clear that elucidating the issue of the second peak requires further separate investigation. At this point we can only offer some preliminary insights into the nature of the second peak that are presented in the next section.

Second Peak. As mentioned earlier, we link the second peak to the formation of small amounts of a different crystalline phase. Our hypothesis takes the following tack. Structurally, silica is an infinite network of corner-linked $(SiO_4)^{4-}$ tetrahedrons. In addition to Si−O−Si oxygens, the surface also features oxygens of Si−O−H groups. As already mentioned, the latter can adsorb ammonium ions by forming $SiO^-NH_4^+$ ionic compounds,[13] whereas the former by forming complexes with Si−O−Si oxygens.[14] Bonding of ammonium ions is likely to be strongest in the $SiO^-NH_4^+$ structures. Among the complexes, stronger bonding should take place when ammonium cations position themselves equidistantly from the three corners of the triangular face of a tetrahedron. In more crowded situation ammonium ions would be more likely to position themselves along the edges of a tetrahedron, giving rise to weaker complexes. While oversimplified, this picture explains that depending on the chemical structures, ammonium ions are going to be bonded to the surface at certain strengths and arranged at certain distances with respect to each other. Different spatial arrangements of ammonia ions can be expected to serve as nuclei for growing somewhat different crystalline lattices of ammonium chloride. Then the lattice that grows from a more stable structure is likely to give rise to more kinetically hindered phase whose phase transition manifests itself as the second DSC peak. The fact that this peak has about 10 times smaller area is indicative of significantly smaller probability of the formation of the respective phase. The probability should then increase with the surface area of individual pores. Since the area increases as the square of the pore diameter, this probability should be significantly larger in larger pores, which is consistent with the observation that the second peak is detected only in ammonium chloride confined to larger (15 and 30 nm) pores. Although our hypothesis can explain the origin of the second peak, its sufficient proof, be it experimental or computational, is yet to be obtained and goes beyond the scope of the present paper.

In order to get further insights into the phase transition process in the nanopores, we have probed its kinetics and compared it against that in the bulk. As mentioned earlier, the shape and position of the DSC peaks suggest that the phase transition in the nanopores is more kinetically hindered than in the bulk. If so, the effect should be quantifiable via kinetic parameters of the process. The phase transition kinetics can be parametrized by extending the approach developed by Vyazovkin and co-workers[37,38] for evaluating the Hoffman−Lauritzen parameters of polymer crystallization kinetics. The first step in this approach is evaluating the effective activation energy, E_α, of a process as a function of the conversion, α, from the amorphous (melt or glass) to crystalline state. Henceforth, the subscript α is used to denote a value related to a given value of conversion. The E_α dependence is estimated by applying an advanced isoconversional method[39] to a set of DSC curves obtained at different temperature programs. The values of α are evaluated as partial areas of a DSC peak. According to this method, for a set of n runs conducted under different temperature programs, $T_i(t)$, the effective activation energy is determined at any given α by finding E_α, which minimizes the function[39]

$$\Psi(E_\alpha) = \sum_{i=1}^{n} \sum_{j\neq i}^{n} \frac{J[E_\alpha, T_i(t_\alpha)]}{J[E_\alpha, T_j(t_\alpha)]} \tag{10}$$

where

$$J[E_\alpha, T_i(t_\alpha)] \equiv \int_{t_{\alpha-\Delta\alpha}}^{t_\alpha} \exp\left[\frac{-E_\alpha}{RT_i(t)}\right] \mathrm{d}t \tag{11}$$

In eq 11, α is varied from $\Delta\alpha$ to $1 - \Delta\alpha$ with a step $\Delta\alpha = m^{-1}$, where m is the number of intervals chosen for computation. The integral, J in eq 11, is estimated by using the trapezoid rule. Minimization is run for each value of α to establish the dependence E_α on α. Unlike the simpler integral isoconversional methods,[40] this method can treat data obtained under arbitrary temperature variation and eliminate a systematic error[39] found when E_α varies significantly with α.

As the next step, the E_α vs α dependence is converted into E_α vs T dependencies that is accomplished by replacing the T_α values obtained at different rates of heating (or cooling) with an average value. Then, the final step involves fitting the experimental E vs T dependence to a theoretical one. In the case of polymer crystallization, a theoretical dependence has been derived[37] from the Hoffman−Lauritzen equation.[41] The latter is an extension of the general condensed phase nucleation model by Turnbull and Fisher[42] which applies to liquid−solid as well as solid−solid transitions. This model can be employed to parametrize the phase transition kinetics in the presently studied systems.

The Turnbull and Fisher equation is commonly written as

dx.doi.org/10.1021/jp403910f | J. Phys. Chem. C XXXX, XXX, XXX−XXX

$$w = w_0 \exp\left(\frac{-\Delta G^*}{RT}\right) \exp\left(\frac{-E_D}{RT}\right) \quad (12)$$

where w is the rate, w_0 is the preexponential factor, R is the gas constant, ΔG^* is the free energy barrier necessary for nucleus formation, and E_D is the activation energy for diffusion of species across the phase boundary. Detailed derivations and expression for the free energy barrier can be found in the texts dealing with crystallization[43] and/or phase transitions.[44] For our purposes, it suffices to note that ΔG^* can be presented as

$$\Delta G^* = \frac{A}{(\Delta T)^2} \quad (13)$$

where A is a constant and ΔT is the supercooling defined as the temperature deviation from the transition temperature, T_{TR}, i.e., $\Delta T = T_{TR} - T$. Equation 13 indicates that the free energy barrier is infinite at T_{TR} and decreases quickly with the supercooling. By substituting eq 13 into eq 12 and recalling that the effective activation energy determined by an isoconversional method is

$$E_\alpha = -R\left(\frac{\mathrm{d} \ln w}{\mathrm{d}T^{-1}}\right)_\alpha \quad (14)$$

one obtains a theoretical E vs T dependence:[45]

$$E_\alpha = E_D - A\left(\frac{2T}{(\Delta T)^3} - \frac{1}{(\Delta T)^2}\right) \quad (15)$$

Note that when transition occurs on cooling below T_{TR}, the value in the parentheses is positive. Since A is normally much larger than E_D, the E_α in eq 15 is negative and its absolute value decreases with decreasing temperature. This has been experimentally demonstrated by applying the advanced isoconversional method to nucleation driven processes taking place on cooling such as crystallization[37,38] and gelation.[46] It must be emphasized that negative values of the effective (i.e., composite) activation energy are not unusual to come across in multistep kinetics.[47] Such values are a mere reflection of the experimental fact that the rate of a process increases with decreasing temperature. Most important is that they can be used to evaluate meaningful energy barriers of the individual kinetic steps as shown in previous publications[37,38] and seen here.

The present kinetic study has been conducted on cooling for two reasons. First, it was reasonable to assume that the cooling data would reveal a larger kinetic effect than the data obtained on heating because the cooling experiments show significantly larger shifts in the DSC peak position, i.e., T_p (Figures 4 and 5). Second, as stated earlier, the transition on heating appears to be limited by thermodynamics rather than kinetics. As a result, the respective DSC peaks shift very little with the heating rate which makes them poorly suitable for isoconversional kinetic analysis.

Kinetic evaluations have been carried for bulk ammonium chloride and ammonium chloride double loaded in 15 nm silica. This particular system has been selected because in it the two DSC peaks observed are well resolved (Figure 6) that allows the respective kinetics to be evaluated independently. In addition to the aforementioned shifts with respect to the bulk sample, one should notice significant amount of noise that is always present in the first peak on cooling. On the contrary, the second peak always appears smooth. At the slowest cooling rate the first peak appears to be followed by a very minor

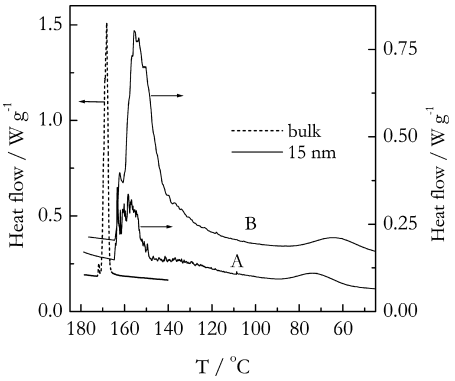

Figure 6. DSC curves measured on cooling for bulk and silica (15 nm pores) loaded samples. Bulk and (A) measured at −2 °C min^{-1} and (B) at −6.75 °C min^{-1}.

exothermic feature at ∼140 °C. Since this feature seems to practically disappear at higher cooling rates, no specific significance was assigned to it in our kinetic analysis. The temperature ranges used for kinetic evaluations have been as follows: 160−175 °C (bulk), 100−170 °C (first peak), and 40−95 °C (second peak). Figure 7 displays the E_α dependencies

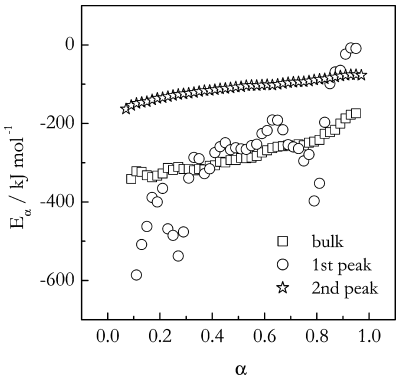

Figure 7. E_α dependencies estimated by means of the advanced isoconversional method.

estimated by applying the advanced isoconversional method to the DSC data collected on cooling. In agreement with the predictions of eq 15 and results obtained for other nucleation driven processes, the E_α values are negative. Although the E_α dependence associated with the first peak is quite noisy due to the noise present in the DSC signal, it is seen that the respective E_α values are closer to the values determined for the phase transition in the bulk than to those estimated from the second peak. This immediately suggests that the two peaks observed in the pores are associated with the processes having significantly different kinetics.

The E_α vs α dependencies (Figure 7) have then been converted to the E_α vs T_α dependencies and fitted to eq 15. The fits have been carried out by taking the onset temperature measured on heating as the T_{TR} value (Table 2). The resulting dependencies and fits are shown in Figure 8. The parameters of the fits are listed in Table 2. Although the correlation coefficient for the first peak is lower than that for the two other fits, all fits are statistically significant. It is remarkable that the size of the diffusion barrier (E_D) in the bulk is similar to the activation energy of ammonium ion self-diffusion in ammonium chloride, 120 ± 10 kJ mol^{-1},[48] as estimated from NMR

dx.doi.org/10.1021/jp403910f | J. Phys. Chem. C XXXX, XXX, XXX−XXX

Table 2. Parameters of Eq 15 Estimated by Fitting the E_α vs T Dependencies

	E_D (kJ mol^{-1})	$A \times 10^{-4}$ (kJ mol^{-1} K^2)	ρ	T_{TR} (°C)
bulk	141 ± 40	0.67 ± 0.06	0.9561	189.6 ± 0.7
1st peak	−14 ± 51	1.5 ± 0.3	0.8629	189 ± 1
2nd peak	22 ± 4	95 ± 3	0.9932	222 ± 1

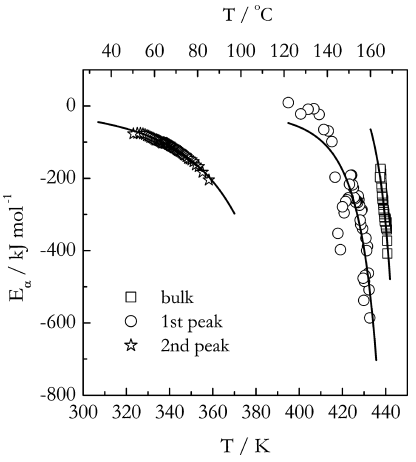

Figure 8. E_α vs T dependencies derived from the E_α dependencies (Figure 7) and fitted to the Turnbull−Fisher model. The lines represent the fits.

measurements. For the process in the pores, the size of this barrier decreases dramatically. Note that it has been reported[49] that the activation energy of ionic self-diffusion in a nanosize solid is markedly lower than in bulk.

However, the most dramatic effect is seen for the parameter A associated with the nucleation barrier. For the process related to the first peak this parameter is 2.5 times larger than that for the process occurring in the bulk. The difference is even larger for the process linked to the second peak, for which the A value is ∼140 times larger than for the bulk.

Now, by using eq 13, we can estimate the temperature dependencies of the free energy barrier to nucleation. These dependencies are shown in Figure 9. The results indicate that in the temperature range of the observed transitions the phase transition in the pores faces markedly larger nucleation barrier than in the bulk. The barrier is especially large for the process related to the second peak. Overall, our kinetics analysis has resulted in two important findings. First, the temperature shifts observed for the processes in the bulk are indeed due to kinetic hindrances and, more specifically, due to increase in the free energy barrier to nucleation. Second, the processes respectively associated with the two DSC peaks have drastically different kinetics as seen from the substantial difference in the nucleation barriers. Note that the second finding is consistent with our hypothesis of the second peak being linked to the transition in some other more stable phase. It should be added that the systems showing two DSC peaks did not demonstrate any unique features in their thermogravimetric curves. That is, the thermal decomposition of ammonium chloride in all loaded systems revealed similar single-step mass loss curves as reported earlier.[12]

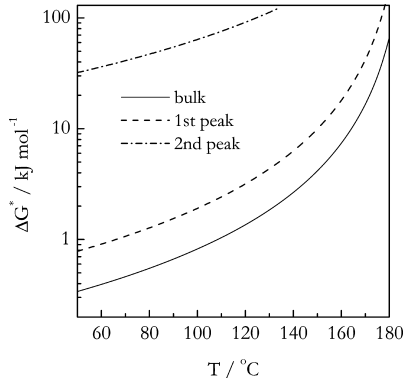

Figure 9. Temperature dependence of the free energy barrier estimated by eq 13.

4. CONCLUSIONS

Our study shows that for ionic compounds loaded from a solution and, thus, filling the silica pores partially the magnitude of the phase transition can be parametrized via the estimated height of the solid layer deposited on the pore wall surface. For the solid−solid transition in ammonium chloride, two major effects have been observed. First, with increasing the layer height, the heat of transition increases toward the bulk value in a manner that suggests the existence of an inactive ionic layer. Second, with decreasing the layer height the transition temperature deviates progressively from the bulk values. More specifically, it gets progressively bigger on heating and progressively smaller on cooling, indicating that the process in the silica nanopores is more kinetically hindered than in bulk. Kinetic analysis reveals that the kinetic hindrance is associated with increasing the size of the free energy barrier to nucleation. An unexpected appearance of the second DSC transition peak is hypothesized to be related to the formation of a different ammonium chloride phase. More work is needed and planned to further explore this phenomenon.

AUTHOR INFORMATION

Corresponding Author

*E-mail: vyazovkin@uab.edu (S.V.).

Notes

The authors declare no competing financial interest.

ACKNOWLEDGMENTS

We gratefully acknowledge the financial support of the National Science Foundation under grant CHE 1052828. We also thank SiliCycle Inc. (Canada) for the generous gift of ultrapure silica gel samples and Mettler-Toledo for donation of the TGA instrument and loaning the DSC instrument used in this study.

REFERENCES

(1) Christenson, H. K. Confinement Effects on Freezing and Melting. *J. Phys.: Condens. Matter* **2001**, *13*, R95−R133.

(2) Alcoutlabi, M.; McKenna, G. B. Effects of Confinement on Material Behaviour at the Nanometre Size Scale. *J. Phys.: Condens. Matter* **2005**, *17*, R461−R524.

(3) Awschalom, D. D.; Warnock, J. Supercooled Liquids and Solids in Porous Glass. *Phys. Rev. B* **1987**, *35*, 6779−6785.

(4) Mu, R.; Malhotra, V. M. Effects of Surface and Physical Confinement on the Phase Transitions of Cyclohexane in Porous Silica. *Phys. Rev. B* **1991**, *44*, 4296−4303.

(5) Pan'kova, S. V.; Poborchii, V. V.; Solov'ev, V. G. The Giant Dielectric Constant of Opal Containing Sodium Nitrate Nanoparticles.

J. Phys.: Condens. Matter **1996**, *8*, L203−L206 (the article devoted to $NaNO_2$ mistakenly called sodium nitrate in the title).
(6) Colla, E. V.; Fokin, A. V.; Koroleva, E. Yu.; Kumzerov, Yu. A.; Vakhrushev, S. B.; Savenko, B. N. Ferroelectric Phase Transitions in Materials Embedded in Porous Media. *Nanostruct. Mater.* **1999**, *12*, 963−966.
(7) Naberzhnov, A.; Fokin, A.; Kumzerov, Yu.; Sotnikov, A.; Vakhrushev, S.; Dorner, B. Structure and Properties of Confined Sodium Nitrate. *Eur. Phys. J. E* **2003**, *12*, S22−S24.
(8) Kutnjak, Z.; Vodopivec, B.; Blinc, R.; Fokin, A. V.; Kumzerov, Y. A.; Vakhrushev, S. B. Calorimetric and Dielectric Studies of Ferroelectric Sodium Nitrate Confined in Nanoscale Porous Glass Matrix. *J. Chem. Phys.* **2005**, *123*, 084708−1−084708−5.
(9) Rysiakiewicz-Pasek, E.; Komar, J.; Cizman, A.; Poprawski, R. Calorimetric Investigations of $NaNO_3$ and $NaNO_2$ Embedded into Porous Glasses. *J. Non-Cryst. Solids* **2010**, *356*, 661−663.
(10) Colla, E. V.; Fokin, A. V.; Kumzerov, Yu. A. Ferroelectrics Properties of Nanosize KDP Particles. *Solid State Commun.* **1997**, *103*, 127−130.
(11) Mu, R.; Jin, F.; Morgan, S. H.; Henderson, D. O.; Silberman, E. The Possible Crossover Effects of $NaNO_3$ in Porous Media: from Bulk to Clusters. *J. Chem. Phys.* **1994**, *100*, 7749−7753.
(12) Farasat, R.; Yancey, B.; Vyazovkin, S. Loading Salts from Solutions into Nanopores: Model and Its Test. *Chem. Phys. Lett.* **2013**, *558*, 72−76.
(13) Iler, R. K. *The Chemistry of Silica*; Wiley: New York, 1979.
(14) Hossain, D.; Pittman, C. U., Jr.; Saebo, S.; Hagelberg, F. Structures, Stabilities, and Electronic Properties of Endo- and Exohedral Complexes of T_{10}-Polyhedral Oligomeric Silsesquioxane Cages. *J. Phys. Chem. C* **2007**, *111*, 6199−6209.
(15) Rao, C. N. R.; Rao, K. J. *Phase Transitions in Solids*; McGraw-Hill: New York, 1978.
(16) Erdey, L.; Gal, S.; Liptay, G. Thermoanalytical Properties of Analytical Grade Reagents. Ammonium Salts. *Talanta* **1964**, *11*, 913−940.
(17) Vyazovkin, S. In *Characterization of Materials*, 2nd ed.; Kaufman, E. N., Ed.; Wiley: New York, 2012; Vol. *1*, pp 471−482.
(18) *CRC Handbook of Thermophysical and Thermochemical Data*; Lide, D. R., Kehiaian, H. V., Eds.; CRC Press: Boca Raton, FL, 1994.
(19) Brinker, C. J.; Scherer, G. W. Sol → Gel → Glass: I. Gelation and Gel Structure. *J. Non-Cryst. Solids* **1985**, *70*, 301−322.
(20) Bourret, A. Low-Density Silica Aerogels Observed by High-Resolution Electron Microscopy. *Europhys. Lett.* **1988**, *6*, 731−737.
(21) Costich, P. S.; Maas, G. J.; Smith, N. O. Transitions in Ammonium Chloride-Ammonium Bromide Solid Solutions. *J. Chem. Eng. Data* **1963**, *8*, 26−27.
(22) Shikano, K.; Katoh, K.; Shimada, S.; Katoh, M. The Effects of Isotopes on Structiural Phase Transition in Ammonium Chloride. *Thermochim. Acta* **1997**, *309*, 153−157.
(23) Rao, K. J.; Rao, C. N. R. Crystal Structure Transformations of Alkali Sulfates, Nitrates, and Related Substances: Thermal Hysteresis in Reversible Transformations. *J. Mater. Sci.* **1966**, *1*, 238−248.
(24) Hamilton, B. D.; Hillmyer, M. A.; Ward, M. D. Glycine Polymorphism in Nanoscale Crystallization Chambers. *Cryst. Growth Des.* **2008**, *8*, 3368−3375.
(25) Ha, J.-M.; Hamilton, B. D.; Hillmyer, M. A.; Ward, M. D. Phase Behavior and Polymorphism of Organic Crystals Confined within Nanoscale Chambers. *Cryst. Growth Des.* **2009**, *9*, 4766−4777.
(26) Rengarajan, G. T.; Enke, D.; Steinhart, M.; Beiner, M. Size-Dependent Growth of Polymorphs in Nanopores and Ostwald's Step Rule of Stages. *Phys. Chem. Chem. Phys.* **2011**, *13*, 21367−21374.
(27) Butterhof, C.; Martin, T.; Ectors, P.; Zahn, D.; Niemietz, P.; Senker, J.; Nather, C.; Breu, J. Thermoanalytical Evidence of Metastable Molecular Defects in Form I of Benzamide. *Cryst. Growth Des.* **2012**, *12*, 5365−5372.
(28) Morf, W. E.; Simon, W. Berechnung von Freien Hydratation-senthalpien und Koordinationszahlen für Kationen aus Leicht Zugänglichen Parametern. *Helv. Chim. Acta* **1971**, *54*, 794−810.
(29) Freund, J. E.; Perles, B. M. *Modern elementary statistics*, 12th ed.; Prentice Hall: Upper Saddle River, NJ, 2006.
(30) Jackson, C. L.; McKenna, G. B. The Melting Behavior of Organic Materials Confined in Porous Solids. *J. Chem. Phys.* **1990**, *93*, 9002−9011.
(31) Marquardt, P.; Gleiter, H. Ferroelectric Phase Transition in Microcrystals. *Phys. Rev. Lett.* **1982**, *48*, 1423−1425.
(32) Saka, H.; Nishikawa, Y.; Imura, T. Melting Temperature of In Particles Embedded in an Al Matrix. *Philos. Mag. A* **1988**, *57*, 895−906.
(33) Grabaek, L.; Bohr, J.; Johnson, E.; Johansen, A.; Sarholt-Kristensen, L.; Andersen, H. H. Superheating and Supercooling of Lead Precipitates in Aluminum. *Phys. Rev. Lett.* **1990**, *64*, 934−937.
(34) Watanabe, A.; Iiyama, T.; Kaneko, K. Melting Temperature Elevation of Benzene Confined in Graphitic Micropores. *Chem. Phys. Lett.* **1999**, *305*, 71−74.
(35) Kaneko, K.; Watanabe, A.; Iiyama, T.; Radhakrishnan, R.; Gubbins, K. E. A Remarkable Elevation of Freezing Temperature of CCl_4 in Graphitic Micropores. *J. Phys. Chem. B* **1999**, *103*, 7061−7063.
(36) Miyahara, M.; Gubbins, K. E. Freezing/Melting Phenomena for Lennard-Jones Methane in Slit Pores: A Monte Carlo Study. *J. Chem. Phys.* **1997**, *106*, 2865−2880.
(37) Vyazovkin, S.; Sbirrazzuoli, N. Isoconversional Approach to Evaluating the Hoffman-Lauritzen Parameters (U* and K_g) from the Overall Rates of Nonisothermal Crystallization. *Macromol. Rapid Commun.* **2004**, *25*, 733−738.
(38) Vyazovkin, S.; Dranca, I. Isoconversional Analysis of Combined Melt and Glass Crystallization Data. *Macromol. Chem. Phys.* **2006**, *207*, 20−25.
(39) Vyazovkin, S. Modification of the Integral Isoconversional Method to Account for Variation in the Activation Energy. *J. Comput. Chem.* **2001**, *22*, 178−183.
(40) Vyazovkin, S. In *The Handbook of Thermal Analysis & Calorimetry*; Brown, M. E., Gallagher, P. K., Eds.; Elsevier: Amsterdam, 2008; Vol. *5*, pp 503−538.
(41) Hoffman, J. D.; Davis, G. T.; Lauritzen Jr., J. I. In *Treatise on Solid State Chemistry*; Hannay, N. B., Ed.; Plenum: New York, 1976; Vol. *3*, p 497.
(42) Turnbull, D.; Fisher, J. C. Rate of Nucleation in Condensed Systems. *J. Chem. Phys.* **1949**, *17*, 71−73.
(43) Mullin, J. W. *Crystallization*, 4th ed.; Elsevier: Amsterdam, 2001.
(44) Papon, P.; Leblond, J.; Meijer, P. H. E. *The Physics of Phase Transitions*; Springer: Berlin, 2002.
(45) Chen, K.; Baker, A. N.; Vyazovkin, S. Concentration Effect on Temperature Dependence of Gelation Rate in Aqueous Solutions of Methylcellulose. *Macromol. Chem. Phys.* **2009**, *210*, 211−216.
(46) Chen, K.; Vyazovkin, S. Temperature Dependence of Sol-Gel Conversion Kinetics in Gelatin-Water System. *Macromol. Biosci.* **2009**, *9*, 383−392.
(47) Atkins, P.; de Paula, J. In *Physical Chemistry*, 9th ed.; W.H. Freeman: New York, 2010; negative activation energies are also discussed in earlier editions, see subject index under "activation energy, negative".
(48) Tansho, M.; Furukawa, Y.; Nakamura, D.; Ikeda, R. Cationic Self-Diffusion in the Highest-Temperature Solid Phases of Ammonium Chloride and Bromide Studied by ^1H NMR. *Ber. Bunsenges. Phys. Chem.* **1992**, *96*, 550−553.
(49) Wilkening, M.; Epp, V.; Feldhoff, A.; Heitjans, P. Tuning the Li Diffusivity of Poor Ionic Conductors by Mechanical Treatment: High Li Conductivity of Strongly Defective $LiTaO_3$ Nanoparticles. *J. Phys. Chem. C* **2008**, *112*, 9291−9300.